International Journal of Biological Macromolecules 47 (2010) 60–67

Contents lists available at ScienceDirect

International Journal of Biological Macromolecules

journal homepage: www.elsevier.com/locate/ijbiomac

Fungicide methyl thiophanate binding at sub-domain IIA of human serum albumin triggers conformational change and protein damage

Quaiser Saquib[a], Abdulaziz A. Al-Khedhairy[a], Saud A. Alarifi[a], Sourabh Dwivedi[a], Jamal Mustafa[b], Javed Musarrat[a,*]

[a] Al-Jeraisy Chair for DNA Research, College of Science, P.O. Box 2455, King Saud University, Riyadh 11451, Saudi Arabia
[b] Chemistry Section, University Polytechnic, AMU, Aligarh 202002, India

ARTICLE INFO

Article history:
Received 7 February 2010
Received in revised form 6 March 2010
Accepted 26 March 2010
Available online 4 April 2010

Keywords:
Human serum albumin
Methyl thiophanate
Fungicide
Fluorescence spectroscopy
Circular dichroism
SDS-PAGE

ABSTRACT

Fluorescence quenching data on interaction of a fungicide methyl thiophanate (MT) with human serum albumin (HSA) elucidated a primary binding site at sub-domain IIA. Stern–Volmer algorithm and double log plot revealed the binding affinity (K_a) and capacity (n) of HSA as $1.65 \times 10^4\ M^{-1}$ and 1.0 ($r^2 = 0.99$), respectively. Cyclic voltammetric and circular dichroism (CD) studies reaffirmed MT–HSA binding and demonstrated reduction in α-helical content of HSA. Substantial release of the carbonyl and acid-soluble amino groups from MT treated HSA suggested protein damage. The plausible mechanism of methyl ($^+CH_3$) group transfer from MT to side chain NH group of tryptophan and HSA degradation elucidates the toxicological and clinical implications of this fungicide.

1. Introduction

Interaction of environmental chemicals with cellular proteins is an important process in understanding their role in inducing the cellular damage and structural alterations in proteins through amino acids modifications [1]. Most of the protein–ligand binding research is primarily focused on investigating the interactions of various natural and synthetic chemicals with HSA, their binding site mapping and characterization [2–4]. A large number of drugs, viz. tetracycline [5], adriamycin [6], indomethacin [7], ibuprofen [8], warfarin [9,8], and diazepam [10], etc. are known to bind with albumin at high affinity binding sites and several sites of much lower affinity, after their administration into the blood stream. Besides, the metals [11], vitamins [12], flavonoids [13], alkaloids [14], many organic dyes and pH indicator substances have also been reported to bind to HSA [15]. However, limited studies are reported in literature on the pesticides as exogenous ligands of HSA [16–18], and the extent and nature of binding of the insecticides, herbicides and fungicides with albumin have not been adequately explored. Silva et al. [17] reported that the organophosphorous pesticide methyl parathion interacts with HSA with an association constant of $3.07 \times 10^4\ M^{-1}$ for the primary binding site close to tryptophan 214 residue. Also, the herbicides (atrazine and 2,4-D) have exhibited the binding constants of $3.5 \times 10^4\ M^{-1}$ and $8.0 \times 10^3\ M^{-1}$ for HSA, and induces major changes in the HSA secondary structure [19]. Our earlier studies on herbicide paraquat–BSA interaction have reported the binding constant (K_a) and binding capacity (n) of albumin as 3.4×10^5 l/mol and 12.9, respectively [16]. Other spectroscopic binding analysis of herbicide paraquat with HSA also demonstrated the paraquat mediated decline in the intrinsic fluorescence of HSA by static quenching and non-radioactive energy transferring [18].

The high-resolution crystal structures indicated that the location of many ligands on serum albumin is still obscure [20,21]. The drug-albumin interaction studies suggested that binding is a reversible process resulting in covalent bond formation affecting the secondary and tertiary structure of albumin [22,23]. Since, the distribution and metabolism of chemical substances in the body are correlated with their affinities towards serum albumin, the investigation with respect to albumin-drug binding is imperative from cytotoxicity endpoint. In this study, a broad spectrum systemic fungicide methyl thiophanate (MT) has been chosen for exploring its interaction with HSA. MT is a known category-III acute inhalation toxicant, likely to be carcinogenic to humans and is widely used for the control of some important fungal diseases of crops [24–26]. It is a potential spindle poison and impairs the polymer-

* Corresponding author at: Al-Jeraisy Chair for DNA Research, Department of Zoology, College of Science, P.O. Box 2455, King Saud University, Riyadh 11451, Saudi Arabia. Tel.: +966 4675768; fax: +966 4675514.
E-mail address: musarratj1@yahoo.com (J. Musarrat).

0141-8130/$ – see front matter © 2010 Elsevier B.V. All rights reserved.
doi:10.1016/j.ijbiomac.2010.03.020

ization of tubulin [27] besides causing delayed cellular proliferation and increase in the frequency of apoptosis. Our recent studies demonstrated its genotoxic potential and capacity to induce DNA strand breaks, micronuclei and 8-oxodG formation in human lymphocytes due to ROS generation in vitro [28,29]. Besides inducing changes in cells, MT has been reported to inhibit certain metabolizing enzymes, including CYP modulation [30] and affect biological cell activities such as synthesis of ATP, signaling, regulation of biosynthetic and catabolic reactions, transport of metabolites and ions [31] due to alteration in the structural and functional integrity of proteins associated with plasma membranes and membranes of intracellular organelles. Lately, Li et al. [32] reported the binding of MT with HSA and speculated its binding at site I on HSA molecule based on computational docking analysis. Nevertheless, the MT–HSA interaction and impact of MT binding on the conformational stability and structural integrity of protein warrants critical and systematic experimental investigations. Thus, in order to assess the magnitude and nature of induced structural damage in HSA, a comprehensive study has been conducted with the aim to determine the (i) extent and nature of interactions of MT with HSA (ii) binding constant (K_a) and number of binding sites (n) on HSA for MT and (iii) MT-induced conformational changes and damage to protein with its plausible mechanism of interaction.

2. Materials and methods

2.1. Materials

Human serum albumin (HSA) fraction V, fatty acid free, acrylamide, N,N′-methylenebisacrylamide, TEMED, low range (6500–66,000 Da) lyophilized protein marker, glycine, bilirubin, dimethyl sulfoxide (DMSO) coomassie brilliant blue R-250, were purchased from Sigma Chemical Company (USA). The methyl thiophanate (dimethyl 4,4′-(o-phenylene)bis(3-thioallophanate), CAS No. 23564-05-8 (97% pure) was a kind gift from Agrochemical Division, Indian Agriculture Research Institute (India). The stock solution of MT (4 mg ml^{-1}) was prepared in DMSO. Tris(hydroxymethyl)aminomethane, tri-carboxylic acid (TCA), ammonium persulfate, glycerol, glacial acetic acid, sodium dodecylsulfate (SDS) and methanol were obtained from Qualigens Fine Chemicals (India). 2,4-dinitrophenylhydrazine, acetophenone and ninhydrin were purchased from s.d. Fine Chemicals (India). 2-Mercaptoethanol was purchased from E. Merck, Darmstadt, (Germany). All experiments were performed using MilliQ water.

2.2. MT–HSA fluorescence measurements

Fluorescence measurements were carried out on a Shimadzu spectrofluorophotometer, model RF5301PC equipped with RF 530XPC instrument control software, at ambient temperature. The fluorescence spectra were measured at a protein concentration of 3.0 μM with a 1 cm path length cell. Excitation and emission slits were set at 3 nm each. The emission spectra were recorded in 290–380 nm range and the excitation wavelength was set at 280 nm, while MT was almost non-fluorescent in this range. All the stock solutions were filtered through 0.45 μm Millipore filters prior to mixing, to minimize the inner filter effect [33]. Fluorescence studies were done by titrating HSA with increasing concentrations of MT. In brief, to a fixed concentration (3.0 μM) of protein solution, varying amounts of MT were added to obtain the desired molar ratios from 1:2 to 1:28. Fluorescence quenching of HSA was determined by the Stern–Volmer equation (1) [34]:

$$\frac{F_0}{F} = 1 + K_{sv}\,[Q] \quad (1)$$

where F_0 and F denote the fluorescence intensities in the absence and presence of quencher (MT), respectively, K_{sv} is the Stern–Volmer quenching constant, and [Q] is the concentration of quencher. Therefore, Eq. (1) was applied to determine K_{sv} by linear regression of a plot of F_0/F vs [Q]. Furthermore, the binding constant (K_a) and number of bound MT to HSA (n) were determined by plotting the double log graph of the fluorescence data using Eq. (2):

$$\log\frac{F_0 - F}{F} \;\text{ vs }\; \log K_a + n\log[Q] \quad (2)$$

Also, the binding constant was calculated from the modified Stern–Volmer equation (3) [35]:

$$\frac{F_0}{\Delta F} = \frac{1}{f_a}K_a[Q] + \frac{1}{f_a} \quad (3)$$

where F_0 and F are the relative fluorescence intensities in absence and presence of the quencher, respectively, $\Delta F = F_0 - F$; f_a is the fraction of the initial fluorophore accessible to the quencher, [Q] the quencher concentration, and K_a is the quenching constant.

2.3. Cyclic voltammetric analysis of MT–HSA binding

The redox potentials of the MT and MT–HSA were determined by cyclic voltammetry in aqueous medium containing 0.4 M KNO_3, as a supporting electrolyte, at room temperature. Cyclic voltammetric experiments were performed using a CH Instruments Electrochemical Analyzer (Japan). A conventional three electrode system was employed with a platinum microcylinder as working electrode, platinum wire as an auxiliary electrode and Ag/AgCl as a reference electrode. The formal potential ($E_{1/2}$) was taken as the average of the anodic (E_{pa}) and cathodic (E_{pc}) peak potentials.

2.4. Site-specific binding of MT on HSA using marker ligands

The specific binding of MT on HSA molecule was studied with bilirubin, which specifically binds to site I on HSA molecule. In this study, HSA was used as fluorescence probe and the changes in fluorescence intensity of HSA bound MT were monitored at 340 nm after excitation at 280 nm upon addition of varying amounts of marker ligands. The percent reduction in fluorescence intensity upon marker ligand binding was calculated considering the fluorescence intensity of MT–HSA complex as 100%.

2.5. Synchronous fluorescence analysis of MT treated HSA

To further determine the induced structural changes in HSA with the addition of MT, synchronous fluorescence analysis has been performed. In brief, the fixed concentration of HSA (3 μM) was titrated with MT at varying molar ratios (1:1–1:10). The wavelength ranges of synchronous scanning were from 310 to 370 nm ($\Delta\lambda$ = 60 nm) and 280 to 330 nm ($\Delta\lambda$ = 15 nm).

2.6. Circular dichroism (CD) measurements

Effect of MT on the native conformation of HSA was analyzed by treating HSA at a fixed concentration of 4.5 μM with 0.1 and 0.2 μM of MT to get the MT–HSA molar ratio of 1:0.02 and 1:0.04. The untreated and MT treated samples were incubated for 2 h in white light at 37 °C. CD measurements were carried out on a Jasco spectropolarimeter, model J-815, Japan. The instrument was calibrated with d-10-camphorsulphonic acid. All the CD measurements were performed at 25 °C with a thermostatically controlled cell holder attached to a NESLAB RTE-110 water bath (NESLAB Instruments, Inc., USA) with an accuracy of ±0.1 °C. Spectra were collected at a scan speed of 100 nm per min with a response

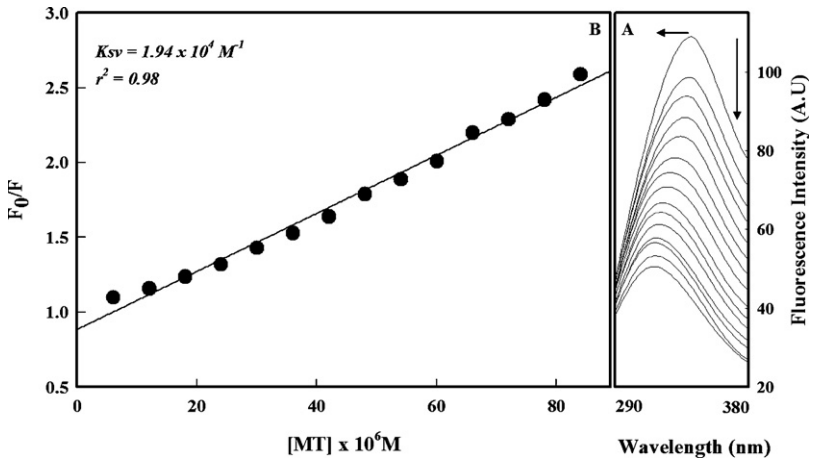

Fig. 1. (A) Fluorescence decay in emission spectra of HSA in the absence (uppermost curve) and presence of increasing amounts of MT. The spectra were obtained in 10 mM Tris–HCl buffer, pH 7.4 at ambient temperature. The molar ratios of MT to HSA were: (top to bottom) 0.0, 2, 4, 6, 8, 10, 12, 14, 16, 18, 20, 22, 24, 26 and 28, respectively. Fluorescence decay is indicated by down arrow (↓) and shift in the emission spectra is shown by horizontal (←) arrow. (B) Stern–Volmer plot describing the fluorescence quenching of HSA by MT at varying molar ratios.

time of 1 s. Each spectrum was the average of four scans. Far-UV CD spectra (200–250 nm) of the untreated and treated HSA were at a 1 mm path length cell. The protein samples for CD measurements were filtered through a Millipore filter (0.45 μM) to remove any suspended material. The results were expressed as mean residue ellipticity (MRE) in deg cm^2 $dmol^{-1}$, which is defined as [MRE = θ_{obs}(mdeg)/10 × n × l × Cp]. The θ_{obs} represents the ellipticity in millidegree, n is the number of amino acid residues (585), l is the path length of the cell in cm and Cp is the mole fraction. The α-helical content of HSA was calculated from the MRE value at 222 nm using the equation % helix = [(MRE222 − 2340)/30,300] × 100 as described by Chen et al. [36].

2.7. SDS-polyacrylamide gel electrophoresis

SDS-polyacrylamide gel electrophoresis of untreated and MT treated HSA was carried out on 10% (w/v) gel, according to the method of Laemmli [37]. In brief, HSA (25 μg) treated with increasing concentrations (1–5 mM) of MT was photoexcited for 2 h at 37 °C. The aliquots (6 μg each) of untreated control and treated protein were loaded on the gel and run at 3 mA per well for 3 h. The gel was stained with coomassie brilliant blue R-250 (0.25%, w/v) and destained with 5% methanol and 7.5% glacial acetic acid at room temperature. Gel was scanned using UVP GelDoc-It imaging system (UVP Ltd., UK) and the staining intensities (densities) of the parent (untreated) and MT treated protein bands were determined with UVP DOC-It LS image analysis software.

2.8. MT-induced degradation of serum albumin

Damage to HSA was assessed by measuring the TCA soluble amino groups according to the method of Moore and Stein [38]. A typical reaction mixture containing HSA (25 μM) and MT in increasing concentrations (200–1000 μM) was exposed to white light for 2 h at 37 °C. The reaction was stopped with the addition of 100 μM EDTA followed by precipitation with 5% (w/v) TCA. Supernatant was obtained after centrifugation at 2500 rpm for 30 min and the acid-soluble amino groups were quantitated using the calibration curve of glycine. Absorbance was read at 570 nm and plotted as a function of MT concentration. The carbonyl groups released from treated serum albumin were also estimated using 2,4-dinitrophenylhydrazine reagent following the procedure of Lappin and Clark [39].

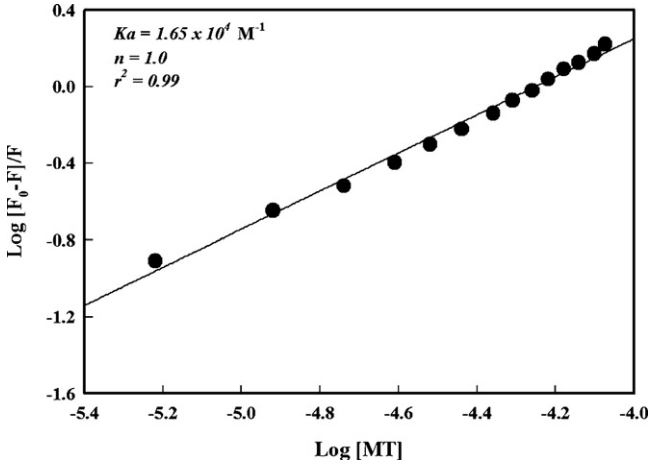

Fig. 2. The double-logarithmic plot of MT–HSA interaction to determine the binding constant (K_a) and number of binding sites (n) on HSA molecule.

3. Results

3.1. Fluorescence quenching of HSA upon MT interaction

Effect of MT on HSA molecule was measured by monitoring the changes in the intrinsic fluorescence of serum albumin at different MT–HSA molar ratios. The fluorescence emission spectra of HSA alone and in presence of varying molar ratios (28:1) of MT–HSA were recorded in the range of 290–380 nm. Fig. 1 A shows the fluorescence decay curves of the free HSA and HSA–MT complex. The titration curves exhibited a pronounced shift of 30 nm towards shorter wavelength in the emission maxima (λ_{em}) of HSA. The fluorescence intensity of MT in the range of 290–380 nm was found to be non-significant as compared with HSA fluorescence. Fig. 1B shows the Stern–Volmer plot of the quenching of HSA fluorescence by MT. The quenching constant (K_{sv}) was determined to be 1.94×10^4 M^{-1} ($r^2 = 0.98$). Based on the double log plot of the fluorescence data, the binding constant (K_a) and number of binding sites (n) on HSA were found to 1.65×10^4 M^{-1} and 1.0 ($r^2 = 0.99$), respectively (Fig. 2). Furthermore, the binding characteristics were revalidated with the modified Stern–Volmer plot of F_0/F vs 1/[Q] (Fig. 3) and the reproducible binding constant has been obtained.

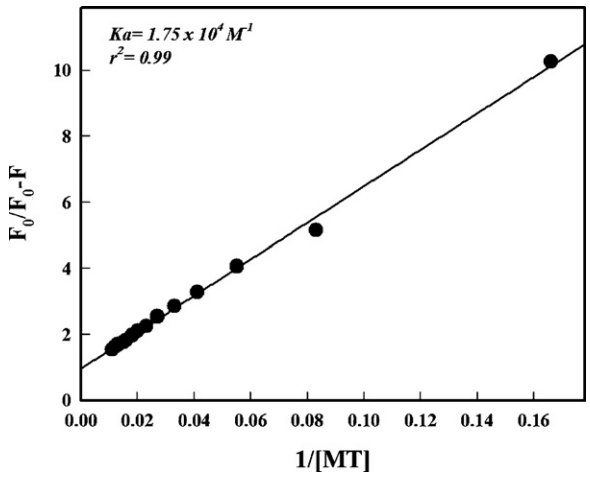

Fig. 3. Modified Stern–Volmer plot of MT–HSA interaction data.

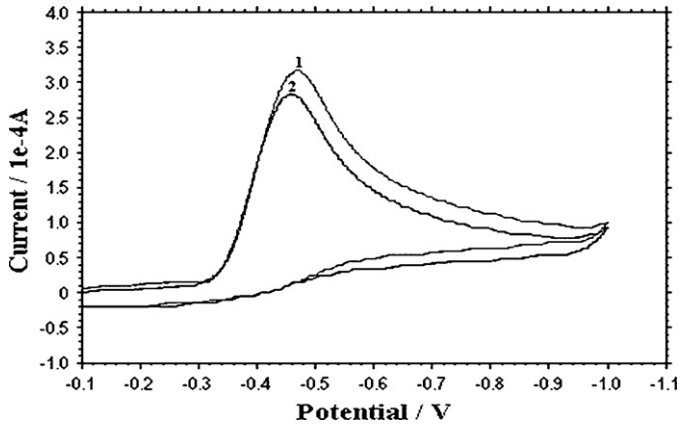

Fig. 4. Cyclic voltammograms showing typical Nernstian behavior at a scan rate of 0.3 V s^{-1}. Curve 1: MT (1 mM); curve 2: MT + HSA (1 mM).

3.2. Cyclic voltammogram of MT–HSA solution

Fig. 4 shows the cyclic voltammograms of MT in the absence and presence of HSA. MT alone (curve 1) exhibited a quasi-reversible peak with an oxidation peak at −0.464 V and a reduction peak at −0.287 V. With the addition of equimolar concentration of HSA (1:1) the cathodic peak current (i_{pc}) of MT decreased from 3.210 to 2.886. The formal potential, E'_0 (or voltammetric $E_{1/2}$) taken as an average of E_{pc} and E_{pa} has been determined to be −0.376 V with MT alone. Addition of HSA to MT solution shifts the E'_0 value from −0.376 V to a lesser negative potential of −0.359 V.

3.3. Site-specific binding of MT on HSA molecule

The competitive displacement of MT from MT–HSA complex with the addition of bilirubin in increasing molar ratios of 1:0.25, 1:0.5 and 1:1 demonstrated the site I specific MT binding on HSA molecule. The emission spectra of MT–HSA complex at 340 nm showed significant reduction in HSA fluorescence upon addition of bilirubin, with a shift of 28 nm in the emission maxima (Fig. 5A). The total percentage decline in fluorescence quenching of MT–HSA complex with the addition of bilirubin has been determined to be 58.12% at 1:1 molar ratio (Fig. 5B). However, the addition of diazepam at the same molar ratios does not exhibit any reduction in the emission spectra of MT–HSA complex (results not shown).

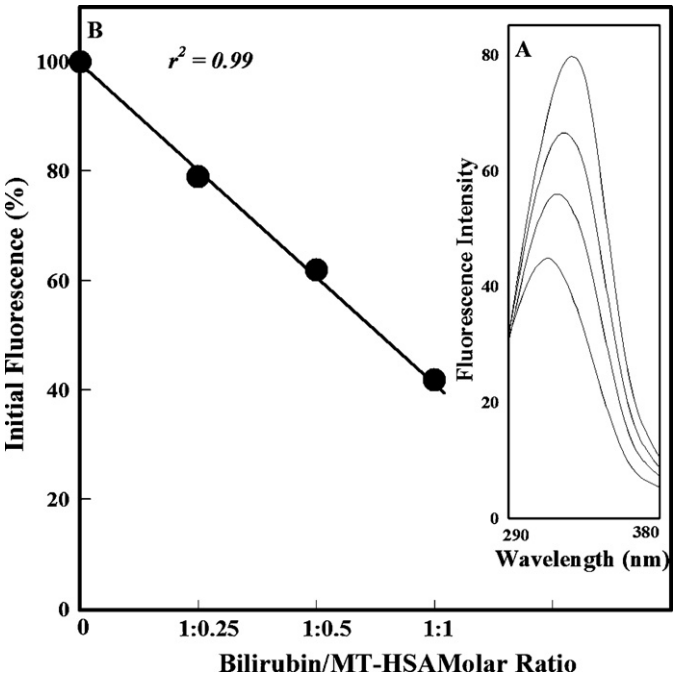

Fig. 5. Panel A (inset) represents the fluorescence quenching of MT–HSA complex with the addition of increasing concentration of bilirubin. Spectra from top to bottom: MT–HSA complex (10:1), bilirubin–HSA molar ratios of 0.25, 0.5 and 1.0. Panel B shows decline in the initial fluorescence of MT–HSA (10:1) complex with the addition of increasing molar ratios of site I marker (bilirubin).

3.4. Conformational changes of HSA upon interaction with MT

Synchronous fluorescence spectra present the information about changes in the molecular microenvironment in vicinity of the fluorophore functional groups. In the synchronous fluorescence of HSA, shift in position of maximum emission wavelength corresponds to the changes of polarity around the fluorophore of amino acid residues. The effect of MT on HSA synchronous fluorescence is shown in Fig. 6A and B. The results in Fig. 6A, reflect that the fluorescence of tyrosine residues is weak and the position of maximum emission wavelength had no change when $\Delta\lambda$ was 15 nm. However, the fluorescence of tryptophan residues was higher and the maximum emission wavelength show a moderate red shift when $\Delta\lambda$ was 60 nm (Fig. 6 B).

3.5. Assessment of structural alterations in HSA upon MT treatment by CD analysis

Titration of HSA with MT has been optimized to achieve the molar ratios of 1:0.02 and 1:0.04 for recording the characteristic HSA spectra. Since MT also absorbs in the spectral range of 200–250 nm at concentrations above 0.1 μM, the lower molar ratios were opted for CD analysis as compared to fluorescence studies, in order to overcome the MT spectral interference without compromising the impact of MT on HSA secondary structure. The spectra of HSA exhibited two negative bands in the ultraviolet region at 209 and 222 nm, characteristic for α-helical structure of protein (Fig. 7). The reasonable explanation is that the negative peaks between 208, 209 and 222–223 nm are contributed to $n \rightarrow \pi^*$ transfer for the peptide bond of α-helix. A concentration dependent change in the ellipticity value has been recorded. The significant reductions in the MRE reflect the alterations in protein helicity. The percent changes in the α-helical content of the protein are shown in Table 1. At a molar ratio of 1:0.04, the perturbation has been determined to be 8% with loss in protein

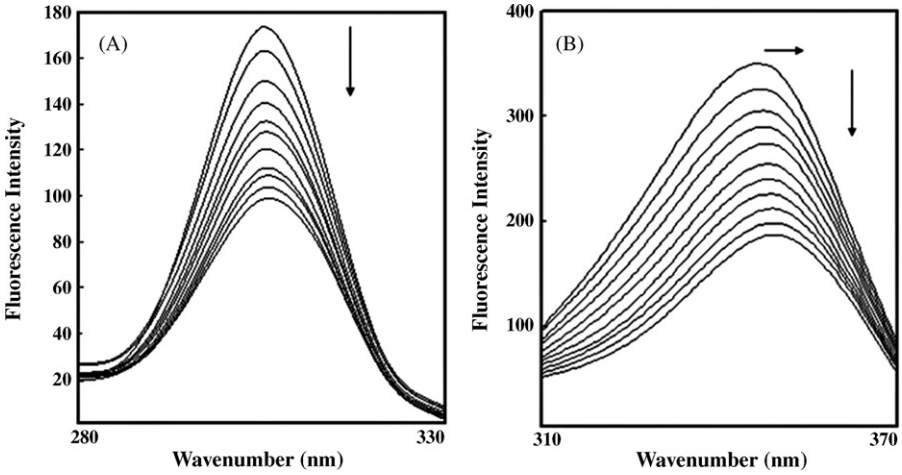

Fig. 6. Synchronous fluorescence spectrum of HSA in absence and presence of MT. (A) $\Delta\lambda = 15$; (B) $\Delta\lambda = 60$. From top to bottom HSA (3.0 μM), MT: 3, 6, 9, 12, 15, 18, 21, 24, 27 and 30 μM, respectively. Fluorescence decay and shift in the emission spectra are indicated by down and horizontal arrows.

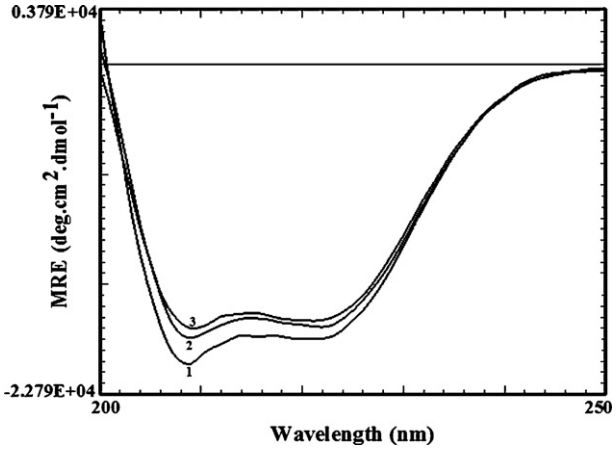

Fig. 7. CD spectra of HSA at different MT concentrations. (1) Free HSA; (2) MT: 0.1 μM; (3) MT: 0.2 μM.

Table 1
Change in relative α-helicity of HSA upon interaction with MT.

HSA–MT molar ratio	MRE_{222} (deg cm^2 dmol^{-1})	α-Helix	%Perturbation
HSA (1:0)	18,950	54.81	–
HSA–MT (1:0.02)	18,142	52.15	5
HSA–MT (1:0.04)	17,670	50.60	8

helicity from 54.8% in native untreated HSA to 50.6% upon MT treatment.

3.6. MT-induced damage in HSA

The quantitative spectrophotometric assays of carbonyl and acid-soluble amino groups released from MT treated HSA indicated the MT-induced HSA damage. Treatment of HSA at the varying concentrations of 200, 400, 600, 800 and 1000 μM of MT for 2 h resulted in the release of 72.2, 129.4, 222.4, 271.8 and 332.1 μM carbonyl groups, respectively (Fig. 8). Also, the increase in absorbance of blue color developed due to acid-soluble amino groups was noticed up to 1000 μM MT at 570 nm. The absolute amount of acid-soluble amino groups released from the MT treated HSA at 200, 400, 600, 800 and 1000 μM were determined to be 1.1, 3.0, 4.1, 5.9 and 7.1 μM, respectively (Fig. 9). Although the protein fragmentation was not apparent on SDS-PAGE at lower concentrations, however, the disappearance of parent bands was noticed at a higher dose range

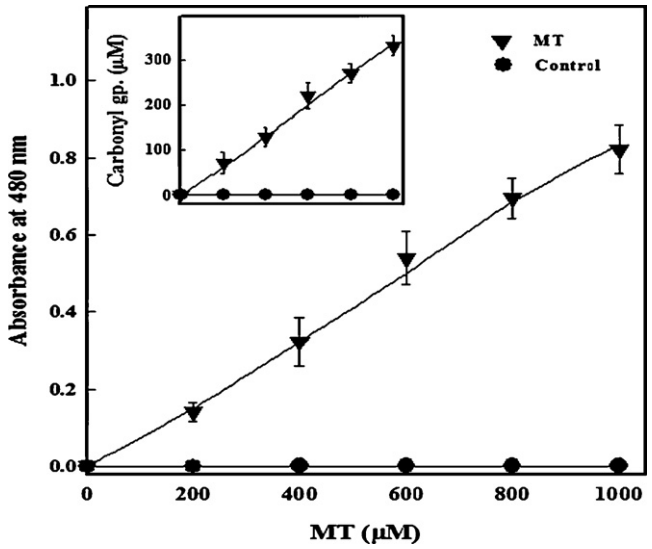

Fig. 8. Carbonyl group released from HSA treated with photosensitized MT for 2 h. The data points represent the mean ± S.D. of three independent experiments done in duplicate.

of 1–5 mM MT, accompanied with some cross-linked products retained on top of the representative gel (Fig. 10A). Furthermore, the densitometric analysis of the bands on the gel revealed a MT concentration dependent decline in the intensity of the HSA bands with 80% loss of band intensity, at 4 mM MT (Fig. 10B).

4. Discussion

Human serum albumin emits strong intrinsic fluorescence at the excitation wavelength of 280 nm, and is sensitive to perturbations in the local surroundings of its microenvironment. Factors such as conformational transition, biomolecular binding and denaturation substantially influence the protein fluorescence [40]. The fluorescence of HSA originates from its aromatic amino acids [41,42], and the intrinsic fluorescence has been used as an indicator of its structural and functional dynamics, to help understand the protein folding and association reactions [14]. In this study, we have explicitly demonstrated the MT-induced conformational changes in the secondary structure of protein through fluorescence and CD analysis. The MT–HSA interaction also triggered the release of protein hydrolysis products indicative of the protein damage, which

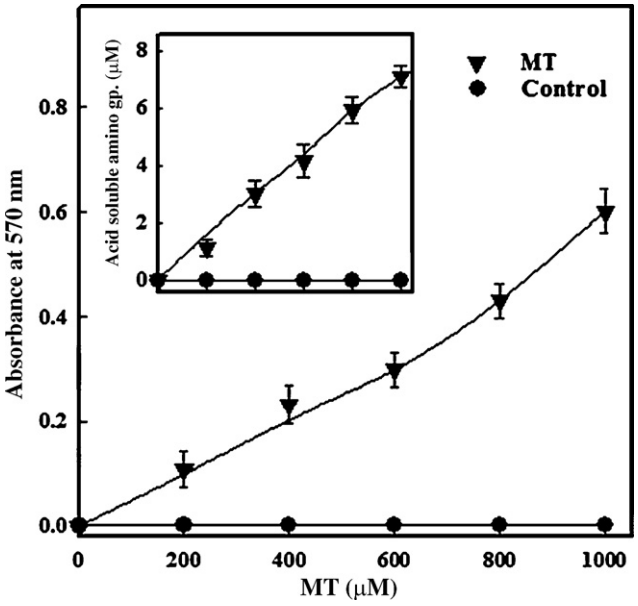

Fig. 9. Photosensitized MT-induced protein fragmentation. HSA was treated with increasing concentration of MT for 2 h and the amount of acid-soluble amino group quantitated. The data represent the mean ± S.D. of three independent experiments done in duplicate.

complements with MT-induced ROS production and DNA damage in vitro in our earlier studies [28,29]. Thus MT–macromolecular interactions may have some reasonable implications from toxicological perspective. Most likely, the pesticides upon assessing the human body interact with the serum proteins. Binding of pesticides to plasma proteins has toxicological importance by controlling their free and active concentrations in the body, thus reducing their time of action [43,44]. Albumin being the most abundant serum protein and a major drug carrier in the blood have more accessibility to bind with such electrophiles and therefore requires in-depth investigation with the aim of determining the extent of binding and consequent molecular damage. Binding of MT with HSA has significantly quenched the intrinsic fluorescence of HSA. The assessment of MT–HSA fluorescence quench titration based on the Stern–Volmer plot of F_0/F vs MT suggest that the quenching could be either dynamic or static quenching. The strong quenching effect accompanied with a prominent shift in emission peak towards the shorter wavelength, as noticed in this study has earlier been reported in HSA with other small ligands [45,46,32]. This could be the effect of changes in microenvironment of aromatic amino acids. The changes around the single tryptophan residue located at 214 position possibly induces conformational deformity in the sub-domain IIA (site I) of HSA molecule, causing loosening of its native structure [47,40,32]. The plausible mechanism of methyl group transfer from MT to NH group of tryptophan upon interaction suggest the formation of dialkylated tryptophan, which may provoke conformational transition in sub-domain II A as depicted in Scheme 1.

The MT stimulated change in the microenvironment around the tryptophan moiety has been further supported by synchronous fluorescence spectroscopic data, which exhibited relatively higher fluorescence quenching of tryptophan residue along with a moderate shift in the emission wavelength. Perturbations within the microenvironment of aromatic amino acids have been assessed by measuring the possible shift in wavelength emission maxima (λ_{max}), which corresponds to the changes of the polarity around the chromophore molecule [48]. When the $\Delta\lambda$ values between excitation and emission wavelength were stabilized at 15 or 60 nm, the synchronous fluorescence provides the characteristic information about the 18 tyrosine and one tryptophan residues [49,50]. Thus, the shift in the emission spectra of synchronous fluorescence validated that MT binds to tryptophan in the hydrophobic cavity and induces structural alterations in HSA, as a consequence the polarity get increased and hydrophobicity get reduced.

Competitive binding of MT–HSA complex with bilirubin as a site I marker exhibited 58.12% reduction in the fluorescence of MT–HSA complex, which has explicitly suggested MT binding at site I on HSA and corroborated the earlier findings [32]. The data has also been validated by cyclic voltammetric analysis, where a significant reduction in the cathodic peak current (ipc) was noticed upon addition of HSA to MT solution. The reduction in peak current could be explained in two possible ways, firstly the HSA interacts with MT to form a non-electrochemical complex, which blocks the electron transfer between the quasi-reversible peaks of MT and electrode, and secondly the competitive adsorption of HSA may occur at the glassy electrode surface, as also suggested by Zhao et al. [51]. The CD analysis has reaffirmed the MT-induced conformational change in secondary structure of HSA even at much lower concentrations of 0.1 and 0.2 μM MT as compared to the amount used in fluorescence based studies. This is the first study on CD based determination of conformational alterations in HSA upon MT–HSA complexation. The MT concentration dependent decrease in band intensities at 209 and 222 nm in the far-UV region suggests a considerable change

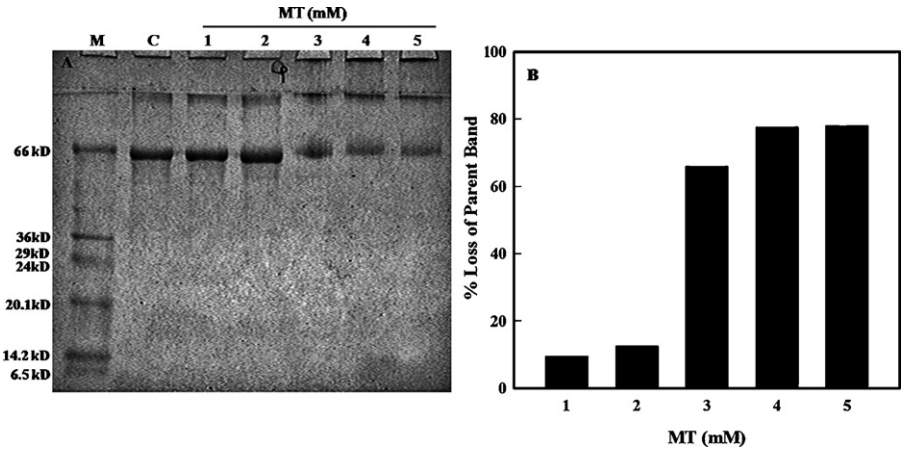

Fig. 10. (A) SDS-PAGE of HSA showing loss of parent band with increasing concentrations of MT. M: molecular size marker; C: untreated control HSA (6 μg); lanes 1–5: HSA treated with 1, 2, 3, 4 and 5 mM of MT, respectively. (B) Histogram represents the densitometric analysis of the HSA bands in lanes 1–5 indicating the loss of parental band with increasing concentrations of MT.

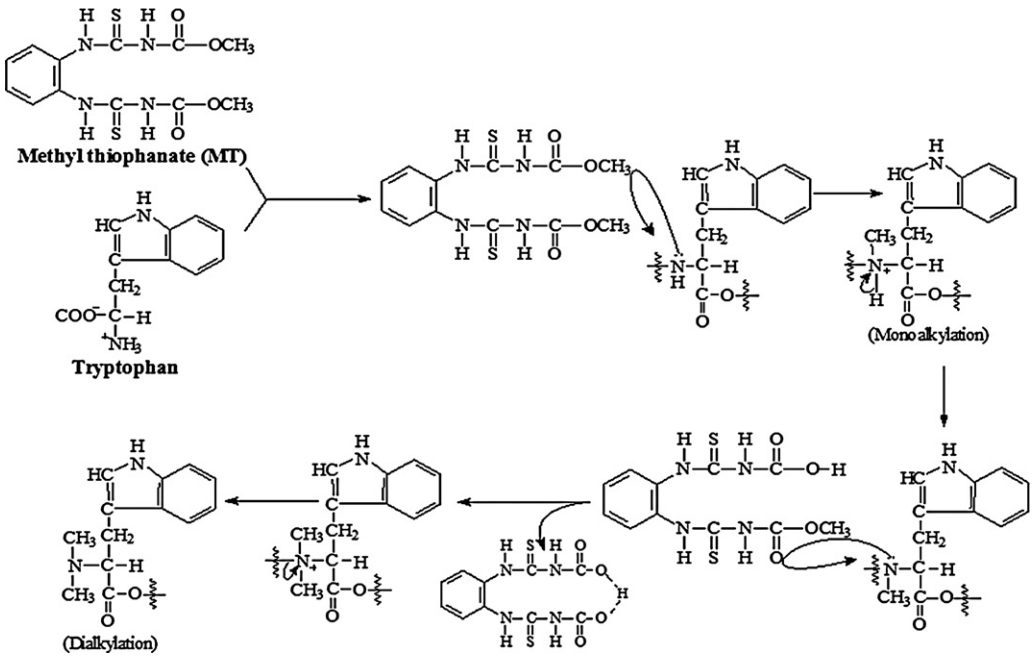

Scheme 1. Proposed mechanism of MT-induced modification of tryptophan.

in the protein secondary structure, primarily due to reduction in α-helical content of treated protein.

The MT-induced protein fragmentation was ascertained by measuring the carbonyl and acid-soluble amino groups as protein degradation markers. The quantitative assessment showed a concentration dependent release of these markers from treated protein in a concentration dependent manner. Since MT mainly interacts with C=O and to a less extent with C–N, therefore, a larger amount of carbonyl groups are released in solution containing treated protein. The protein degradation may be due to peptide bond hydrolysis and/or chain scission at α-carbon position. The densitometric analysis of HSA bands on gel revealed a gradual MT concentration dependent decline in the intensity. No evidence was obtained for the presence of discrete fragments, however, the reaction of MT with HSA results in the loss of the parent protein via the formation of small random fragments, which corroborates with the results of Hawkins and Davies [52] who have also reported the disappearance of HSA bands at much higher (150- and 200-fold) concentration of hypochlorite (HOCl) in SDS-PAGE analysis. It is likely that the MT-induced HSA damage observed in the form of its degradation products could be due to its significant binding and/or generation of free radicals in vicinity of protein upon photoexcitation, as demonstrated in our earlier studies on MT-induced ROS production and macromolecular damage [28,29].

5. Conclusions

In conclusion, the fluorescence quench titration suggested strong binding affinity of HSA for MT. The interaction mainly occurs with aromatic amino acids, preferably the tryptophan moiety on sub-domain IIA due to the alkyl group transfer from MT to amino acid functional group. The proposed mechanism (Scheme 1) suggests that the amino group of tryptophan possessing free lone pair of electrons may act as a nucleophile. It attacks the alkyl cation and facilitate the release of ($^{+}CH_3$) group from MT to side chain NH group of tryptophan on HSA. Consequently, the HSA containing dialkylated tryptophan at subdomain II A may undergo structural changes. Thus, the critical MT–HSA binding and the tendency of MT to generate reactive oxygen species as reported in our earlier studies, renders the serum albumin vulnerable to progressive degradation as demonstrated with the release of carbonyl and acid-soluble amino groups from MT treated HSA. Also, the interaction of MT with the physiologically important carrier protein HSA entails pesticide toxicity and stipulates the possibility of developing pesticide-specific biosensors for human biomonitoring and health risk assessment.

Acknowledgment

Financial support through the Abdul Rahman Al-Jeraisy Chair for DNA Research, King Saud University, Riyadh, KSA, is greatly acknowledged.

References

[1] U.A. Boelsterli, Drug Metab. Rev. 25 (1993) 395–451.
[2] S. Curry, H. Mandelkow, P. Brick, N. Franks, Nat. Struct. Biol. 5 (1998) 827–835.
[3] A.A. Bhattacharya, T. Grune, S. Curry, J. Mol. Biol. 303 (2000) 721–732.
[4] B.X. Huang, C. Dass, H.Y. Kim, Biochem. J. 387 (2005) 695–702.
[5] M.A. Khan, S. Muzammil, J. Biochem. Mol. Biol. Int. 46 (1998) 943–950.
[6] L. Trynda-Lemiesz, H. Kozlowski, Bioorg. Med. Chem. 4 (1996) 1709–1713.
[7] V.D. Trivedi, H. Vorum, B. Honore, M.A. Qasim, J. Pharm. Pharmacol. 51 (1999) 591–600.
[8] G. Fanali, P. Ascenzi, M. Fasano, Biophys. Chem. 129 (2007) 29–35.
[9] G. Sudlow, D.J. Birkett, D.N. Wade, Mol. Pharmacol. 11 (1975) 824–832.
[10] W.E. Muller, U. Wollert, Pharmacology 19 (1979) 59–67.
[11] H. Liang, C.Q. Tu, H.Z. Zhang, X.C. Shen, Y.Q. Zhou, P.W. Shen, Chin. J. Chem. 18 (2000) 35–41.
[12] E. Karnaukhova, Biochem. Pharmacol. 73 (2007) 901–910.
[13] C.D. Kanakis, P.A. Tarantilis, M.G. Polissiou, S. Diamantoglou, H.A. Tajmir-Riahi, J. Mol. Struct. 798 (2006) 69–74.
[14] Y.Q. Wang, H.M. Zhang, G.C. Zhang, J. Pharm. Biomed. Anal. 41 (2006) 1041–1046.
[15] Y.J. Hu, W. Li, Y. Liu, J.X. Dong, S.S. Qu, J. Pharm. Biomed. Anal. 39 (2005) 740–745.
[16] R. Jaiswal, M.A. Khan, J. Musarrat, J. Photochem. Photobiol. B 67 (2002) 163–170.
[17] D. Silva, C.M. Cortez, J.C. Bastos, Toxicol. Lett. 147 (2004) 53–61.
[18] G. Zhang, Y. Wang, H. Zhang, S. Tang, W. Tao, Pest. Biochem. Physiol. 87 (2007) 23–29.
[19] M. Purcell, J.F. Neault, H. Malonga, H. Arakawa, R. Carpentier, H.A. Tajmir-Riahi, Biochim. Biophys. Acta 1548 (2001) 129–138.
[20] X.M. He, D.C. Carter, Nature 358 (1992) 209–215.
[21] S. Curry, P. Brick, N. Franks, Biochim. Biophys. Acta 1441 (1999) 131–140.
[22] T. Peters Jr., All About Albumin, Biochemistry, Genetics, and Medical Applications, Academic Press, San Diego, 1996.
[23] T.O. Hushcha, A.I. Luik, Y.N. Naboka, Talanta 53 (2000) 29–34.

[24] Proposed Guidelines for Carcinogen Risk Assessment, Office of Research and Development U.S. Environmental Protection Agency Washington, DC EPA/600/P-92/003C, Federal Register 61 (79) (1996) 17960–18011.
[25] K.A. Hassall, The Biochemistry and Uses of Pesticides, second ed., Macmillan Press Ltd, 1990.
[26] M.E. Traina, P. Fazzi, C. Macri, C. Ricciardi, A.V. Stazi, E. Urbani, A. Mantovani, J. Appl. Toxicol. 18 (1998) 241–248.
[27] F. Maranghi, C. Marcri, C. Ricciardi, A.V. Stazi, M. Resci, A. Mantovani, Reprod. Toxicol. 17 (2003) 617–623.
[28] Q. Saquib, A.A. Al-Khedhairy, S. Al-Arifi1, A. Dhawan, J. Musarrat, Toxicol. In Vitro 23 (2009) 848–854.
[29] Q. Saquib, A.A. Al-Khedhairy, B.R. Singh, J.M. Arif, J. Musarrat, J. Environ. Sci. Health (B) 45 (2010) 1–6.
[30] M. Paolini, L. Pozzetti, P. Perocco, M. Mazzullo, G.C. Forti, Cancer Lett. 135 (1999) 203–213.
[31] C.M. Palmeira, A.J. Moreno, B. Vasco, V.C. Madeira, Med. Sci. Res. 25 (1997) 339–342.
[32] J. Li, X. Liu, C. Ren, J. Li, F. Sheng, Z. Hu, J. Photochem. Photobiol. B 94 (2009) 158–163.
[33] C.F. Chignell, in: C.F. Chignell (Ed.), Methods in Pharmacology, vol. 2, Appleton-Century-Crofts, New York, 1972, pp. 33–62.
[34] J.R. Lakowicz, Principles of Fluorescence Spectroscopy, second ed., Plenum Press, New York, 1999.
[35] J.R. Lakowicz, Principles of Fluorescence Spectroscopy, third ed., Springer, New York, 2006.
[36] Y.H. Chen, J.T. Yang, H.M. Martinez, Biochemistry 11 (1972) 4120–4131.
[37] U.K. Laemmli, Nature 227 (1970) 680–685.
[38] S. Moore, W.H. Stein, J. Biol. Chem. 211 (1954) 907–913.
[39] G.R. Lappin, L.C. Clark, Anal. Chem. 23 (1951) 541–542.
[40] J.L. Yuan, Z. Iv, Z.G. Liu, Z. Hu, G.L. Zou, J. Photochem. Photobiol. A 191 (2007) 104–113.
[41] D. Li, J. Zhu, J. Jin, X. Yao, J. Mol. Struct. 846 (2007) 34–41.
[42] A. Sulkowska, J. Mol. Struct. 616 (2002) 227–232.
[43] U. Kragh-Hansen, Pham. Rev. 33 (1981) 17–53.
[44] T. Cszerhárti, E. Forgács, J. Chromatogr. A 699 (1995) 285–290.
[45] W. He, Y. Li, J. Tian, H. Liu, Z. Hu, X. Chen, J. Photochem. Photobiol. A 174 (2005) 53–61.
[46] B. Zhou, Z.D. Qi, Q. Xiao, J.X. Dong, Y.Z. Zhang, Y. Liu, J. Biochem. Biophys. Methods 70 (2007) 743–747.
[47] L. Trynda-Lemiesz, B.K. Keppler, H. Koztowski, J. Inorg. Biochem. 73 (1999) 123–128.
[48] T. Yuan, A.M. Weljie, H.J. Vogel, Biochemistry 37 (1998) 3187–3195.
[49] J. Tang, F. Luan, X. Chen, Bioorg. Med. Chem. 14 (2006) 3210–3217.
[50] W.C. Abert, W.M. Gregory, G.S. Allan, Anal. Biochem. 213 (1993) 407–413.
[51] J. Zhao, X. Zheng, W. Xing, J. Huang, G. Li, Int. J. Mol. Sci. 8 (2007) 42–50.
[52] C.L. Hawkins, M.J. Davies, Biochem. J. 340 (1999) 539–548.